Supplementary Methods:

Clinical Studies:

In the first study, 18 volunteers (7 males; 11 females) were enrolled in the Clinical and Translational Research Center (CTRC) for entry into a randomized, double blind, cross - over comparison of placebo or 81mg aspirin orally administered each day for 5 days. Urine were collected for analysis on baseline of day 1 prior to the first dose and for the intervals of -2-0; 0-2; 2-4; 4-6; 6-8; 8-12; 12-16; 16-24 hours pre or post the fifth dose on day 5. After a 10-day washout the same procedures were followed with whichever treatment they did not receive during the first period. Urine was stored at -80 °C.

In the second study, patients assigned for elective PTCA were considered for inclusion in the study. Three groups of patients were enrolled. Patients who had a history of allergy to aspirin were treated with clopidogrel and abciximab, but not aspirin. Patients who had been on low dose aspirin (81mg/day) at entry to the study were continued on this regimen. Patients who had been on aspirin 325mg/day were continued on this regimen. All aspirin treated patients had been on that regimen for a minimum of 5 days prior to PTCA. Most patients presenting for PTCA electively were on the higher dose of aspirin. Urinary samples were collected 6 hours prior to procedure.

In the third study, 9 healthy volunteers (6 males; 3 females) were screened at the CTRC for entry into the randomized, double blind, cross - over comparison of placebo with aspirin 81mg for each of 5 days with a single dose of niacin 600 mg administered 30 minutes after the last dose of aspirin/placebo (day 5) or 24 hours after the last dose of aspirin/placebo (day 6). There was a two week washout period between each treatment.

Urine was collected before aspirin and niacin dosing -2-0, and 0-2hr, 2-4hr, 4-6hr, 6-12hr and 12-24hr after aspirin and niacin dosing for prostaglandins metabolites.

Animals:

COX-2 knock out mice were purchased from Jackson Labs and were generated on a mixed C57BL/6 X 129S7/SvEvBrd-Hprt genetic background (50%:50%) as previously described(1).COX-1 knock down mice were generated on a mixed C57BL/6 X 129S6/SvEvTac genetic background (50%:50%) as previously described (2). The DP1 KOs were a kind gift from Dr. Shuh Narumiya of the University of Kyoto. DP1 KO (C57BL/6J and Sv129) mice were intercrossed with fully backcrossed LDLR KOs for the atherosclerosis studies and with fully backcrossed ApoE KOs for the aneurysm studies. Both strains were on a mixed background (C57BL/6J and Sv129), backcrossed to the 7^{th} generation. Hence, littermate controls were used in both sets of studies. For thombogenesis and blood pressure measurement by telemetry we used fully backcrossed DP1 KOs to C57BL/6J and WT controls.

Blood pressure measurement by telemetry:

Male WT and DP1 KO 8-12 weeks old, were used for blood pressure telemetry measurements at baseline and after 2 weeks on a 4% high salt diet (Harlan Teklad, TD.92034) by telemetry using PA-C20 telemetry probes (Data Sciences International).

Atherosclerosis:

At 8 weeks of age, littermate controls (LDLR KO and DP1-LDLR dKOs) were fed a western diet (Taklad Harland, TD 88137) for 12, 24 and 36 weeks. Atherosclerotic plaque burden was determined by the en face method, using Sudan red IV (Sigma-Aldrich) staining on aortas cut open longitudinally from the aortic root to the femoral

bifurcation. The stained aortas were pinned onto black wax prior to plaque quantification. Images were photographed and digitized by using the Image Pro analysis system (version 6). Atherosclerosis was quantified by comparing the *en face* positive stained area with total surface area of the aorta.

Prostaglandin Measurements:

Urine was collected for 12 hours before and after intra peritoneal injection of niacin (300mg/kg body weight) in COX-1 knock down and COX-2 knockout mice and their controls. For the platelet depletion experiments, either an anti-platelet antibody (Emfret, catalog # R300) or vehicle was administered into the circulation of male C57BL56 mice via retro-orbital injection at a dose of 3μg/g body weight. Mice were given 24 hours to recover during which time period urine was collected. 24 hours later, a separate urine was collected for 12 hours followed by niacin (300mg/kg body weight) or vehicle via intraperitoneal injection and urine was then collected for a further 12 hours for prostaglandin analysis.

Flow Cytometry:

Allophycocyanin (APC)-conjugated rat antihuman HM74A/GPR109A antibody (Catalog: FAB2760A) and its immunoglobulin subtype control (Catalog: MAB0061) were purchased from R & D systems. Platelet-rich plasma (PRP) was obtained and diluted to concentration of $1x10^7$/ml with platelet-poor plasma (PPP). 10μL of APC-conjugated HM74A reagent was added to 100μL PRP. Following 40 minutes incubation, 900μL tyrode's buffer was added to the system for final flow cytometric analysis.

Immunofluorescence:

Platelets were added to fibrinogen precoated 8-well chamber slides (BD Falcon), and then treated with vehicle or nicotinic acid. Platelets were fixed with 3.7 % formaldehyde then permeabilized with 0.2% Triton X-100 in PBS. The GPR 109A receptor was visualized using a primary goat anti-niacin receptor antibody (Santa Cruz, sc-48537) and secondary rabbit anti-goat antibody conjugated to Alexa Fluor 488 (Molecular Probes). Another stain involved a primary rabbit anti-niacin receptor antibody (Bioworld # BS2605) and secondary goat anti-rabbit antibody conjugated to Alexa Fluor 488 (Molecular Probes). In addition, platelet CD-61 integrin β3 was visualized using a primary mouse antibody (Santa Cruz) and secondary donkey anti-mouse conjugated to Alexa Fluor 555 (Molecular Probes). Slides were mounted in Permount® (Fisher Scientific).

cAMP assay:

LANCE cAMP kit was used as previously described(3). Briefly, Platelets (platelet rich plasma, PRP), were pre-incubated with vehicle or nicotinic acid for 10 min at 37°C, were mixed with anti-cAMP antibody conjugated to Alexa Fluor 647, then treated with vehicle or forskolin for 30 min at room temperature, adding a detection reagent containing Europium-Streptavidin-Biotin cAMP was added. Time resolved TR-FRET was performed 1h later using an EnVision 2103 Multilabel Reader (PerkinElmer).

Immunoprecipitation of lPGDS:

Immunoprecipitation was carried out using a system purchased from Santa Cruz (Protein A/G PLUS-Agarose, #sc-2003). Agarose beads (0.5ml) were washed three times and coated with human lPGDS monoclonal antibody (60µg; Cayman #10004342) or the subtype of IgG control (60µg; Biolegend, Rat IgG1, κ) and incubated for one hour. After

triple wash by PBS, 1 ml of platelet poor plasma obtained from healthy volunteers was added and incubated for one hour. Then after centrifugation, the pellet was lysed for western blotting and the supernatant plasma was used to re-suspend fresh platelets obtained from the same subject.

Western blotting:

GPR109A: Briefly, PRP from healthy volunteers was incubated for 10 min with or without 100 or 1000 μM niacin, and then washed twice with ice-cold PBS containing complete protease inhibitor mixture. Washed platelet (WPs) were treated by brief sonication and then centrifuged at 3000 × g for 5 min to remove unbroken cells and nuclear fractions (whole platelets fraction). Subsequently, one aliquot of the supernatant was centrifuged at 21,000 × g for 30 min to separate the membrane and cytosolic fractions. The proteins in the cytosolic fraction were precipitated with 70% ethanol, and both pellets were resuspended in PBS. Proteins in the whole platelet, membrane and the cytosolic fractions were electrophoresed on a 10% SDS-polyacrylamide gel, transferred to nitrocellulose, and immunoblotted using goat polyclonal anti-HM74 (1:100, Santa Cruz Biotechnology) or rabbit polyclonal anti-HM74 (1:100, Bioworld) and next probed with horseradish peroxidase-labeled secondary antibodies, and chemiluminescence was detected using horseradish peroxidase-substrate (Amersham). The blots were stripped and reprobed using an anti-β-actin (1:5000, Sigma) monoclonal antibody as a control for protein loading.

lPGDS: The agarose pellet was lysed by 10 minutes heating at 90 °C. Proteins in the lysate were electrophoresed on a 10% SDS-polyacrylamide gel, transferred to nitrocellulose, and immunoblotted using rat monoclonal anti-lPGDS (1:200,

Cayman10004342) and next probed with horseradish peroxidase-labeled secondary antibodies, and chemiluminescence was detected using horseradish peroxidase-substrate (Amersham).

mRNA expression of prostanoid receptors by RT-PCR on isolated platelets from human and mouse:

Platelet rich plasma (PRP) was isolated from mice as described (4): Blood was taken from vena cava from sedated mice with a syringe containing 50 µl 3.8% trisodium citrate (37°C) and was diluted 1:1 with Tyrodes buffer (20 mM HEPES, 140 mM NaCl, 5 mM $MgCl_2$, and 5 mM KCl, pH 7.4) and trisodium citrate and was adjusted to a final concentration of 0.38%. While human blood was collected in citrate coated sample glass from healthy volunteers and was then diluted 1:1 in Tyrode buffer and adjusted with trisodium citrate. PRP was isolated by centrifugation at 800 rpm for 5 min at room temperature (without brakes). PRP was carefully removed to avoid leukocyte contamination and EDTA was added to a final concentration of 7.7 mM. Then platelets were isolated by centrifugation at 2000 rpm for 10 min and the platelet pellet was washed in PBS before RNA was isolated by trizol isolation according to manufacturer's instructions (Ambion Life Technologies). 1 µg total RNA was used for cDNA synthesis was made using iScript cDNA synthesis kit (BioRad). 50ng cDNA was used for DP1, TP, EP3 and GAPDH by RT-PCR (33 cycles,30 sec at 95°C, 30 sec at 60°C, and 30 sec at 72°C). As a positive control we used cDNA from ilenum in mice and brain and renal cortex in humans. Primer sequences used were as follows: for mDP1; forward: 5'-TGG-CTC-TCA-TGA-CAG-TGC-TC-3', and reverse: 5'-CAA-GGC-TTG-GAG-GTC-TTC-TG-3'; for mTP: forward: 5'-GAC-TGC-GAG-GTG-GAG-ATG-AT-3', and reverse: 5'-

ATG-ACA-GGT-GGT-GTC-TGC-AA-5'; for mGAPDH: forward: 5'-TGA-TGG-CAT-GGA-CTG-TGG-3', and reverse: 5'-CAG-CAA-TGC-ATC-CTG-CAC-3'; for mEP3: Forward: 5'- AGC-TCA-TGG-GGA-TCA-TGT-GT-3', and reverse: 5'- TTG-CAC-TCC-TTC-TCC-TTT-CC-3'; for hDP1: Forward: 5'-TGA-TGA-CCG-TGC-TCT-TCA-CT-3', and reverse: 5'-CAA-AGG-GTC-CAC-AAT-TGA-AA-3'; for hTP: Forward: 5'-AGG-TGG-AGA-TGA-TGG-CTC-AG-3', and reverse: 5'- CGG-CGG-AAC-AGG-ATA-TAC-AC-3'; for hGAPDH: Forward: 5'-CGA-GAT-CCC-TCC-AAA-ATC-AA-3', and reverse: 5'-GTC-TTC-TGG-GTG-GCA-GTG-AT-3'.

Platelet disaggregation in mouse whole blood:

Freshly isolated heparinized (Sigma) whole blood was taken from the vena cava and samples were diluted 1:4 in prewarmed physiologic saline solution prior to measurement of aggregation after stimulation with 10 μM ADP under constant stirring at 37 °C. When maximal platelet aggregation was attained, either PGD_2 (1.4 μM), PGD_2 (14 μM) or the IP agonist cicaprost (10 nM) were added to determine the effect on disaggregation.

Immunohistochemistry of DP1 on human atherosclerotic lesions:

Human mammary arteries with and without atherosclerotic lesions were obtained [after prior individual consent and approval of the protocol from a local independent ethical review board at Region Southern Denmark (ref: S-20100044)] from patients undergoing coronary bypass operations. Formalin fixed tissues were stained for DP1. The paraffin embedded vessels were cut in 5 μm sections, deparaffinized and hydrated, then the sections were demasked by 20 min incubation in citrate buffer, pH6 (DAKO) at 97°C. After several washes in tris-buffered Saline containing 0.05% Tween 20 (TBST), the sections were incubated with CSAII Peroxidase Reagent, rinsed, blocked with CSAII

Blocking Solution, then incubated with polyclonal DP1 antibody (4 μg/ml, Cayman chemical) diluted in Antibody Diluent (DAKO) for 30 min. As a negative control we used a non-specific rabbit IgG (4 μg/ml, DAKO). After several washes in TBST the sections were incubated with CSA II HRP-conjugated-anti rabbit-IgG diluted 1:5, rinsed in TBST, then incubated with CSA II Amplification Reagent, rinsed, and then incubated with CSAII Anti-Fluorescence-HRP according to manufacturer's instructions(DAKO). DP1 positive staining was visualized with CSA II DAB Chromogen for 5 min and counter stained with Mayer's hematoxylin and mounted with aquatex. Pictures were captured with a Sony DP50 camera on a BX51 Olympus microscope.

Supplementary Figures:

Suppl. Fig 1. Formation of PGD_2 from human platelet and effect of PGD_2 on human platelet

(A) TxB_2 production in vitro by human platelets after aggregation stimulated by 10 μM adenosine 5'-diphosphate (ADP), 10 μM arachidonic acid (AA), 10 μM collagen (CA) and 10 μM Thrombin Receptor-Activating Peptide (TRAP). Pretreatment with 100 μM aspirin for 10 minutes prior to addition of the platelet agonist completely suppressed production of TxB_2. (n=4 for each group)

(**B)** Pretreatment with PGD_2 (100nM) for 5 minutes prior to addition of ADP (10 μM) abolished ADP induced platelet aggregation (Y axis indicates percent of light transmission)

Suppl. Fig 2. Expression of eicosanoid receptors on mouse and human platelets

The thromboxane receptor (TP) is expressed on both mouse (n = 5, **A**) and human platelets (n=2, **B**) as measured by RT-PCR. DP1 is expressed on human platelets (**A**), but not those of the mouse (**A**). In mouse platelets we also detected EP3 receptor (**A**) as described by Ma et al(4), which could explain the additional pro-aggregatory effect seen with high dose PGD_2 (**D)** (5). In freshly isolated and heparinized whole blood samples, platelets were stimulated to aggregate with 10 μM ADP. When maximal platelet aggregation was attained, either PGD_2 (1.4 μM, **c**), PGD_2 (14 μM, **D**) or the IP agonist cicaprost (10 nM, **E**) were added to determine their effect on platelet disaggregation. Panels (**C-E)** shows original traces with arrows indicating the time when each reagent was added and the aggregation response expressed on the Y axis as units of impedance (ohm). While PGD_2 failed to disaggregate mouse platelets (**F, G**), unlike the response observed in human platelets, disaggregation was readily observed (**H**) in response to the IP agonist, cicaprost (n=4; *, $p<0.05$).

Suppl. Fig. 3. DP1 deletion augments Ang II induced hypertension in hyperlipidemic mice

(A) Mean systolic blood pressure in 8-10 week old male ApoE mice (n= 27-22) and DP1-ApoE dKO (n= 26-18) on a western diet at baseline and during the following 4 weeks (wk) of chronic Ang II infusion measured by non invasive tail cuff measurements. Mean systolic blood pressure is significantly increased by Ang II infusion (# ,$p<0.05$) and after 4 weeks of Ang II infusion mean systolic blood pressure were significantly elevated in DP1-ApoE dKOs vs. ApoE KOs at the end of 4 weeks of Ang II infusion (*, $p<0.05$). (**B)** Shows the intergroup systolic blood pressure variations of the individual mice at baseline

and after 4 weeks of Ang II between the 2 groups. (**C, D)** Both systolic blood pressure and mean arterial blood pressure (*, $p < 0.001$) were significantly increased after 14 days of 4% high salt feeding in both normolipidemic DP1 KO males and WT (*, $p<0.001$) mice, but there was no difference between genotypes at baseline on a regular rodent chow (NSD, 0.7% NaCl) or in response to the high salt diet (HSD, 4 % NaCl).

Sppl. Fig. 4. Modest proatherogenic impact of DP1 deletion in female hyperlipidemic mice

(**A, B)** Representative en face aortas from each time point and each genotype from female and male mice. Each aortic depiction is assembled from 3 individual picture frames (magnified 8 times). (**C**) Plaque burden, as assessed by en face quantification of the percentage of total aorta area (n= 11-17) was significantly augmented by DP1 deletion in female mice (** ,$p< 0.01$ by 2-way ANOVA). **(D**) While plaque burden increased with time in male mice (n=10-14; $p<0.001$ by 2 way ANOVA), there was no significant effect of genotype.

Suppl. Fig. 5. DP1 localization in human mammary artery with and without atherosclerotic plaque.

DP1 is localized to vascular human endothelial cells in mammary arteries without evident atherosclerosis (A-C). DP1 is associated in atherosclerotic plaque with cells most likely to be macrophages or intravascular endothelial cells (D-H). In some, but not all sections DP1 was also associated with vascular smooth muscle cells (G+H). We used a non-specific rabbit antibody as a negative control (I). Complete arrows indicate intravascular DP1 positive endothelial cells. Truncated arrowheads indicate intravascular DP1 positive

myeloid cells which co-localize with CD68 positive cells in serial sections (data not shown). Scale bar indicates 50 μm (B, C, E, F, and H) and 200 μm (A, D, G, and I).

Suppl. Fig. 6. Niacin evokes platelet COX-1 dependent prostaglandin formation in mice

COX-1 knockdown significantly ($p<0.001$; n=5 in both groups) and completely suppressed PGDM (**A**) and TxM (**B**), both at baseline and in response to niacin. While basal urinary PGEM(**C**) and PGIM(**D**) were unaltered, the niacin evoked increase in both of these metabolites was also significantly blunted (** = $p<0.01$) by COX-1 knock down. COX-2 deletion failed to suppress significantly basal or niacin evoked increases in any metabolite (**E-H**; n=5 in each group). Depletion of platelets (n=8 for vehicle and n=9 for antibody injected mice) suppressed significantly (* = $p<0.05$) the niacin evoked increase in TxM and PGDM, but not in PGIM or PGEM induced responses (**I-L**).

Suppl. Fig 7. Transient increase of prostaglandin formation post administration of anti-GPIb alpha antibody to induce platelet depletion in mice

Urine was collected for the first 24 hours immediate after the injection of the anti-GPIb alpha antibody. Urinary PGDM (**A**) and TxM (**B**) both increased compared to baseline, suggesting platelet activation after antibody injection, prior to their depletion.

Suppl. Fig. 8 Expression of the GPR109A receptor on human platelets

(**A**) Representative of 3 experiments on distinct human donor blood of GPR109A detection on platelets by flow cytometery (gray background indicates IgG isotope control staining, while blue trace indicates anti GPR109A antibody staining). (**B**) Representative

of 3 experiments showing immunofluorescence staining of the GPR-109A receptor on human platelets. Platelets were co-stained with beta-intergrin 3 and GPR-109A. Red staining indicates beta-intergrin3; green staining indicates GPR-109A (Santa Cruz, sc-48537). Morphologically, GPR109A is expressed more on the cell membrane rather than in the cytosol. (**C**) GPR-109A receptor immunofluorescence staining by another antibody (Bioworld # BS2605), no counter stain of beta-integrin 3.

(**D**) Representative Western blot showing the effect of niacin stimulation of platelets in 3 experiments resulting in degradation of the receptor in the membrane fraction. GPR109A is constantly expressed on the cell membrane and in the cytosol. Niacin treatment decreased its expression on cell membranes while increasing the expression of the receptor degradation product (bands sizes suggested in the antibody datasheet). (**E**) Niacin induces a dose dependent decrease in platelet cAMP reflected by an inverse LANCE signal. Experiments were performed on blood from three donors, with triplicates at each dose of niacin. Triplicate experiments were performed at each dose of niacin.

Suppl. Fig. 9. Immunodepletion of l-PGDS suppresses PGD_2 production in human platelet rich plasma

(**A**) Western blot shows l-PGDS protein in the lysate of beads coated with human l-PGDS monoclonal antibody or the same subtype of the IgG control. (**B**) Suppressed production of PGD_2 from aggregated platelets stimulated by ADP (10μM) when platelets were re-suspended in lPGDS immunoprecipitated plasma.

Suppl. Fig. 10. DP1 dependent platelet inhibition by Niacin

(**A**) Niacin (100μM) suppressed the spreading induced by a low dose of ADP (10 μM), Pretreatment with the DP1 antagonist, MK 0524 prevented this niacin effect (**B**).

Suppl. Fig. 11. Effect of Niacin on human platelets

Schematic representation of platelet signaling. Niacin (NA) activates the GPR 109A niacin receptor (NR) which couples to Gi and potentially restrains cAMP production, while facilitating Gq dependent platelet activation by agonists such as ADP and TxA_2. Activation of the Gs coupled DP1 by PGD_2 either directly inhibits platelet activation or restrains these pathways, offseting the results of NR activation.

References

1. Dinchuk, J.E., Car, B.D., Focht, R.J., Johnston, J.J., Jaffee, B.D., Covington, M.B., Contel, N.R., Eng, V.M., Collins, R.J., Czerniak, P.M., et al. 1995. Renal abnormalities and an altered inflammatory response in mice lacking cyclooxygenase II. *Nature* 378:406-409.
2. Cheng, Y., Wang, M., Yu, Y., Lawson, J., Funk, C.D., and FitzGerald, G.A. 2006. Cyclooxygenases, microsomal prostaglandin E synthase-1, and cardiovascular function. *J Clin Invest* 116:1391-1399.
3. Xia, M., Huang, R., Guo, V., Southall, N., Cho, M.H., Inglese, J., Austin, C.P., and Nirenberg, M. 2009. Identification of compounds that potentiate CREB signaling as possible enhancers of long-term memory. *Proc Natl Acad Sci U S A* 106:2412-2417.
4. Ma, H., Hara, A., Xiao, C.Y., Okada, Y., Takahata, O., Nakaya, K., Sugimoto, Y., Ichikawa, A., Narumiya, S., and Ushikubi, F. 2001. Increased bleeding tendency and decreased susceptibility to thromboembolism in mice lacking the prostaglandin E receptor subtype EP(3). *Circulation* 104:1176-1180.

5. Abramovitz, M., Adam, M., Boie, Y., Carriere, M., Denis, D., Godbout, C., Lamontagne, S., Rochette, C., Sawyer, N., Tremblay, N.M., et al. 2000. The utilization of recombinant prostanoid receptors to determine the affinities and selectivities of prostaglandins and related analogs. *Biochim Biophys Acta* 1483:285-293.

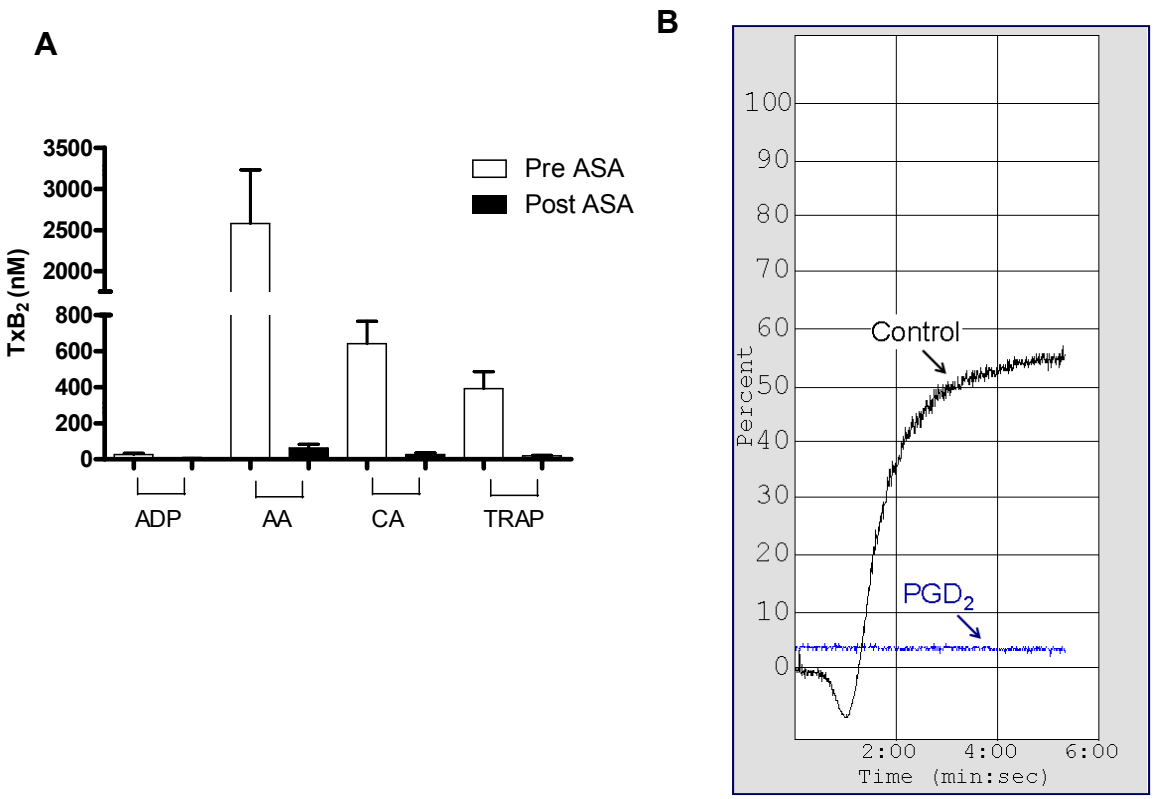

Supplement Fig 1. Formation of PGD_2 from human platelet and effect of PGD_2 on human platelet

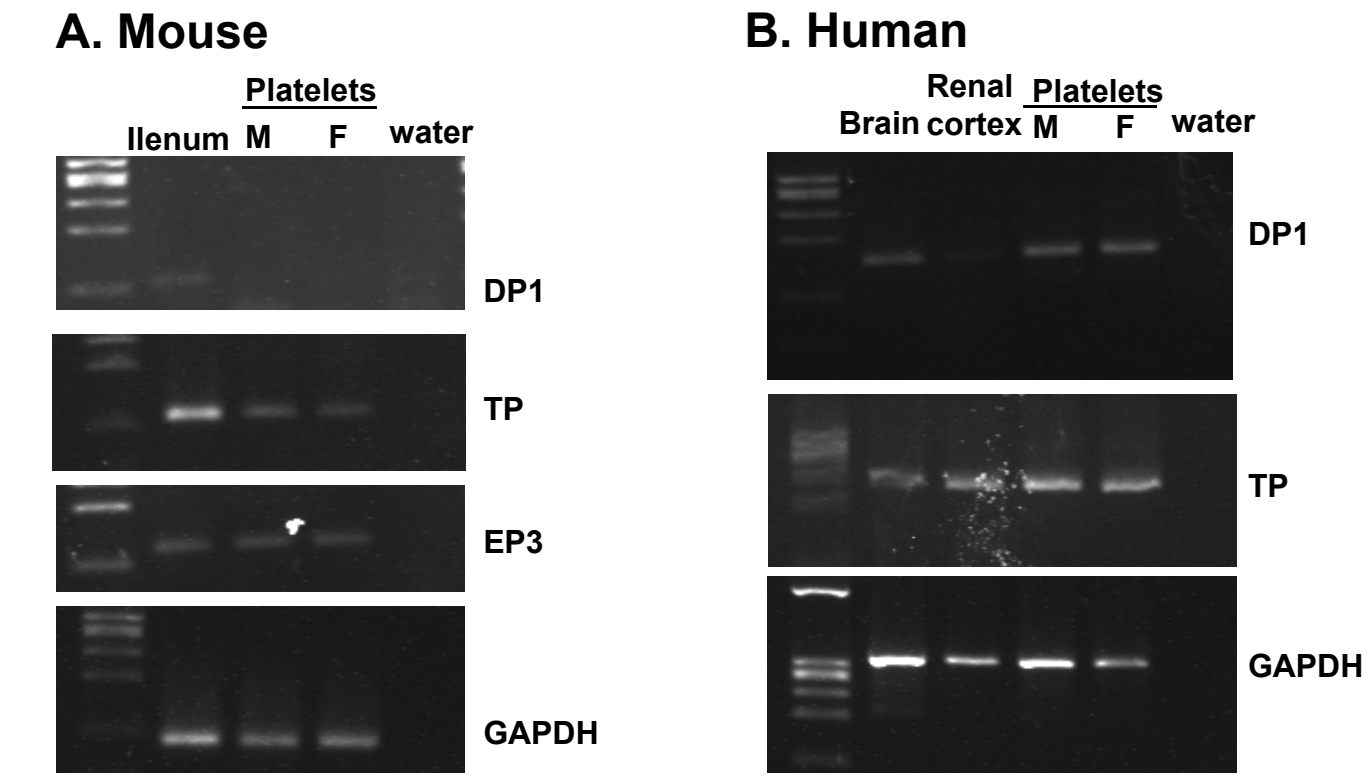

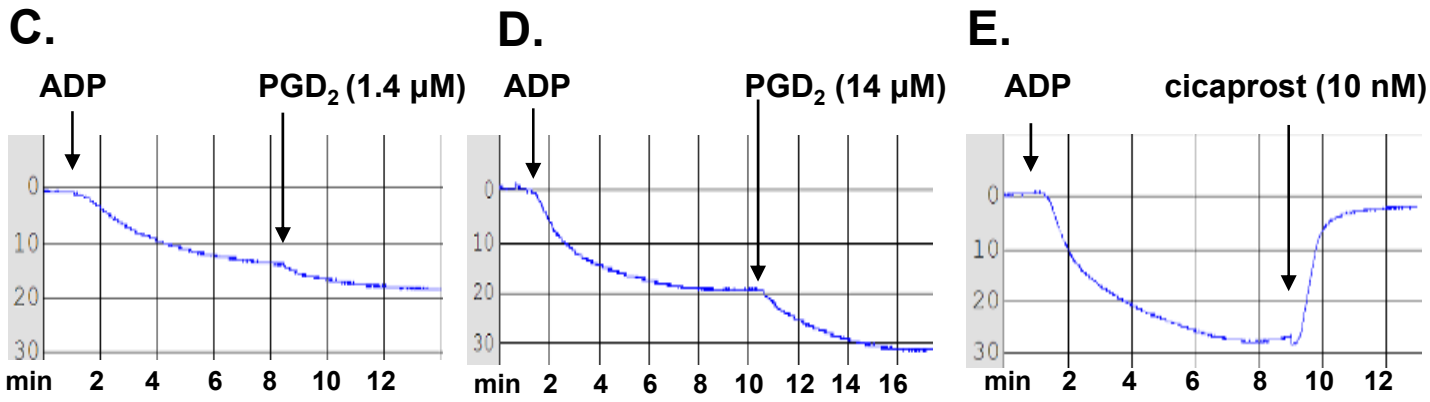

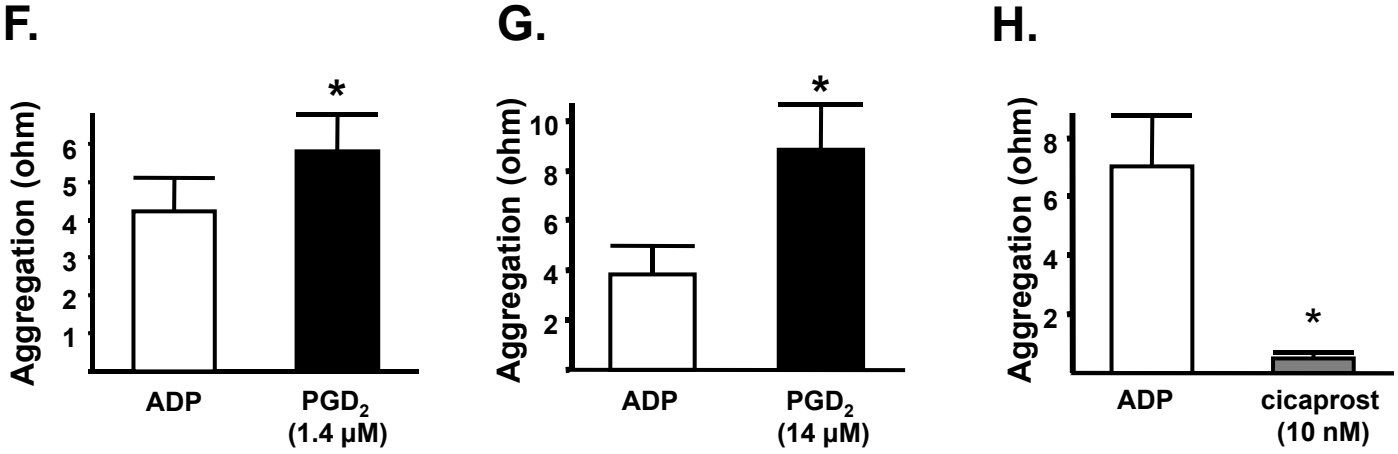

Supplement Fig 2. TP and DP1 expression on platelets in mouse and humans

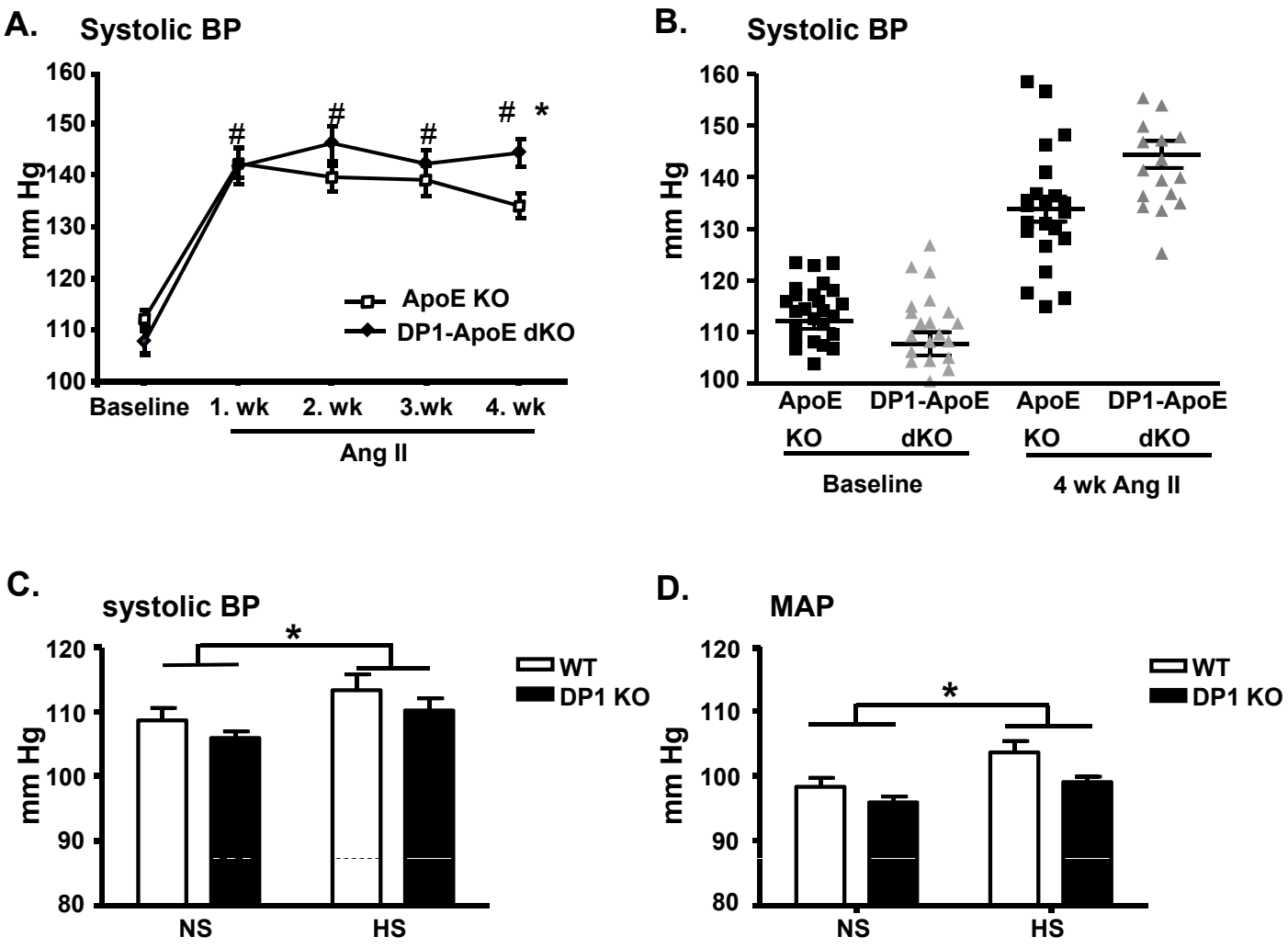

Supplement Fig 3.DP1 deletion augments AII induced hypertension in hyperlipidemic mice but high salt intake has no effect on normolipidemic DP1 KO mice

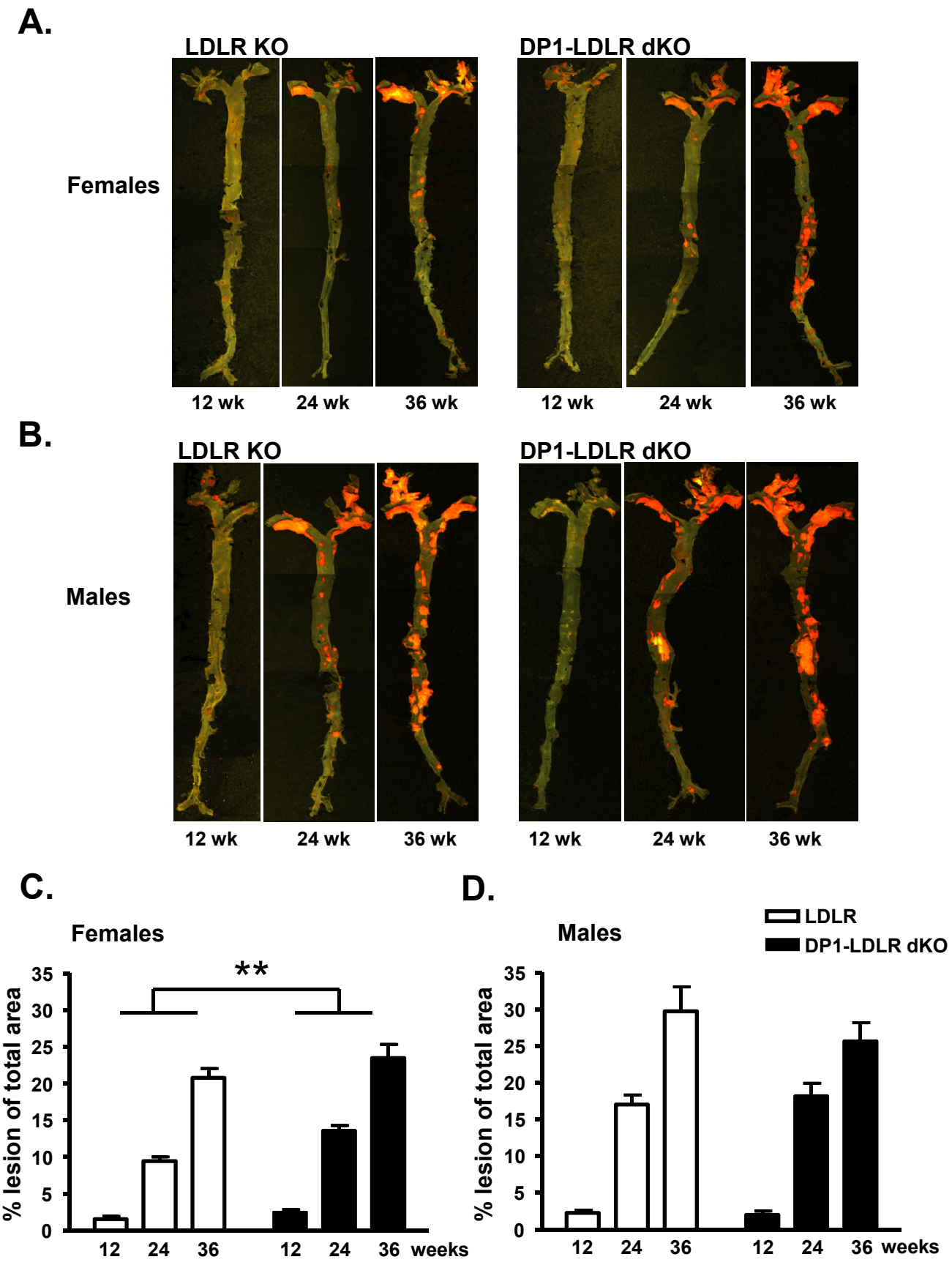

Supplement Fig 4. Modest proatherogenic impact of DP1 deletion in female hyperlipidemic mice

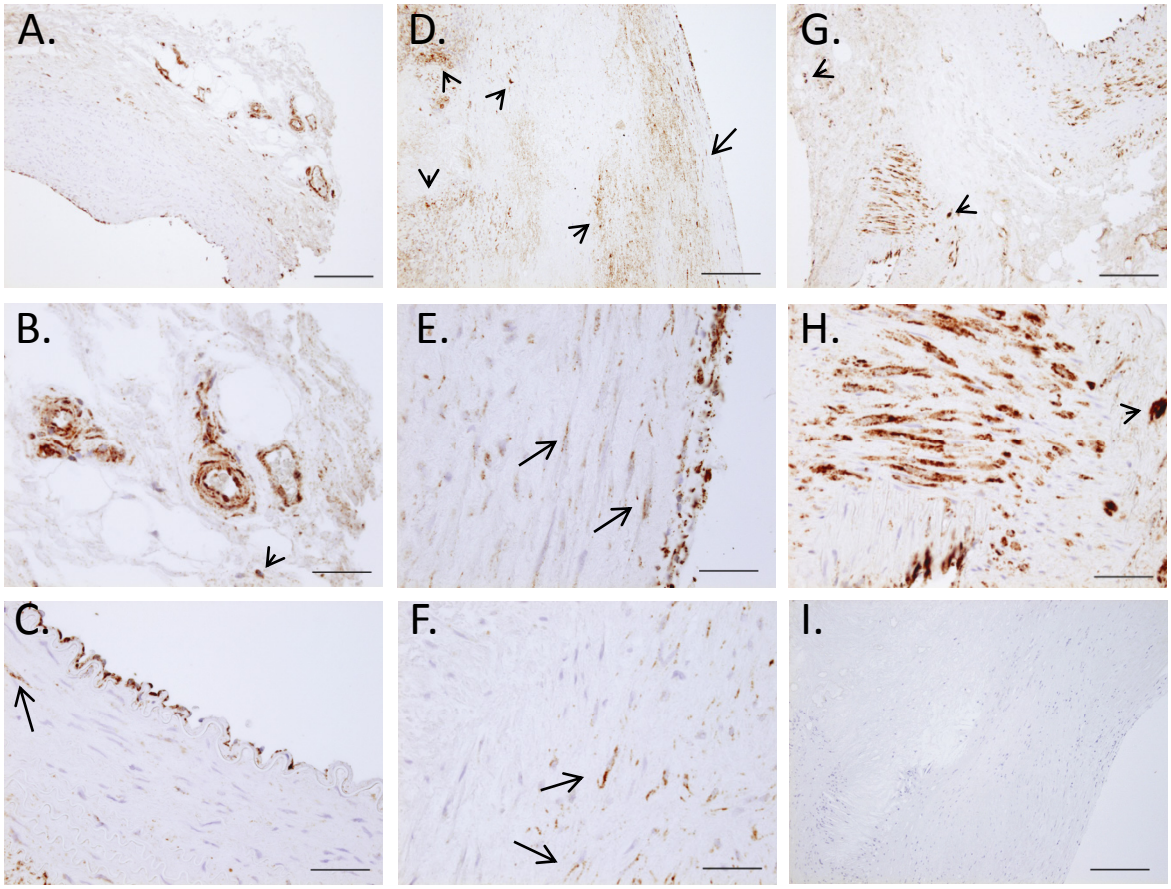

Supplement Fig 5. DP1 localization in human mammary arteries with and without atheroma

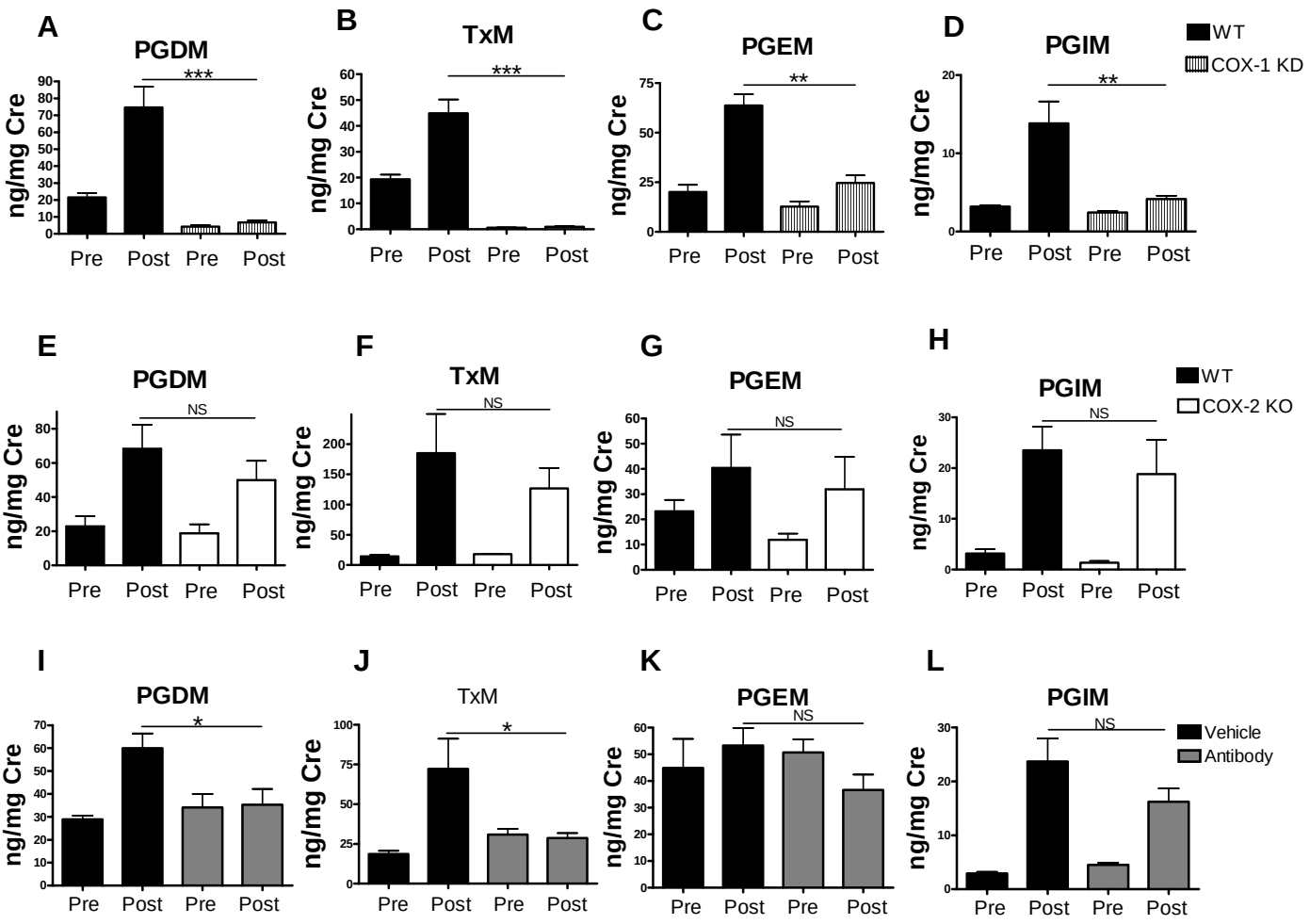

Supplement Fig 6. Niacin evokes platelet COX1 dependent prostaglandin formation in mice

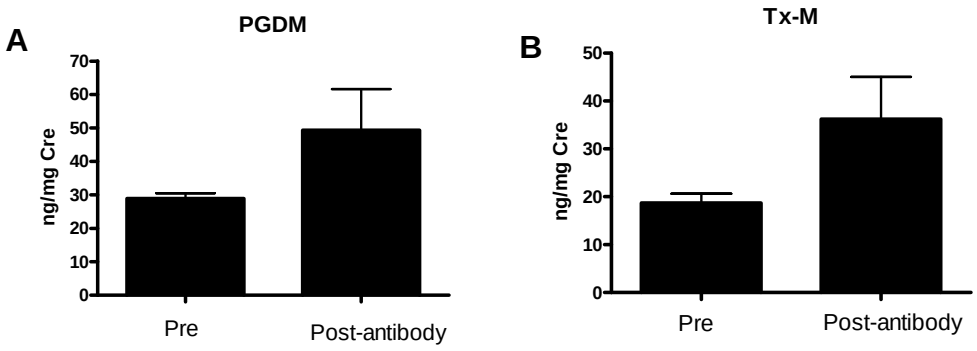

Supplement Fig 7. Transient increase of prostaglandins immediately post administration of antibody to induce platelet depletion in mice

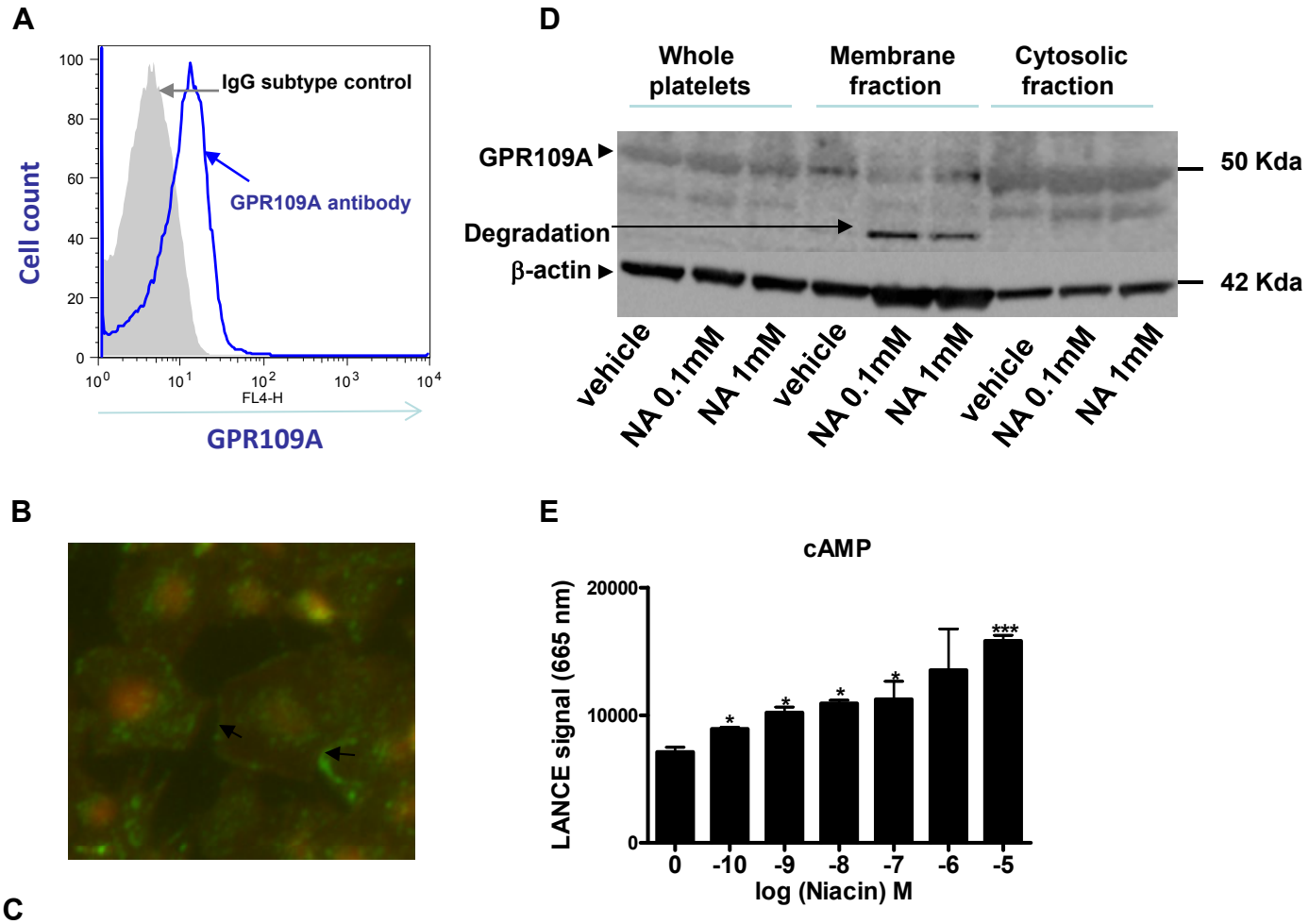

Supplement Fig 8 Expression of the GPR109A receptor on human platelets

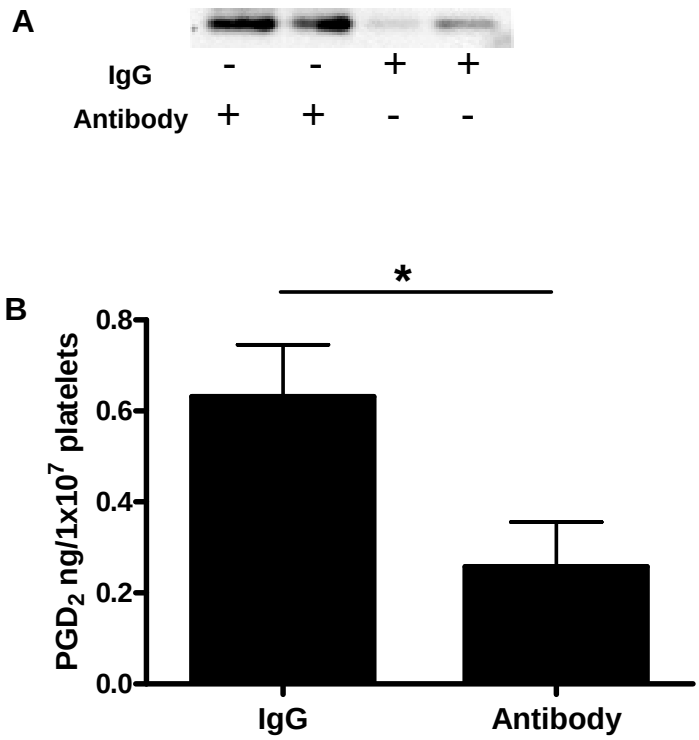

Supplement Fig 9. Immunodepletion of l-PGDS suppresses PGD_2 production in human platelet rich plasma

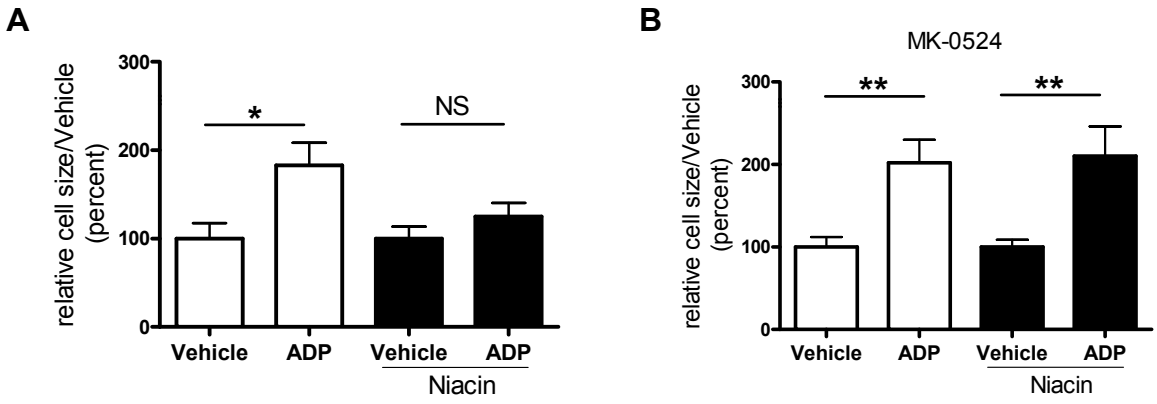

Supplement Fig 10. Effect of DP1 antagonist on platelet spreading

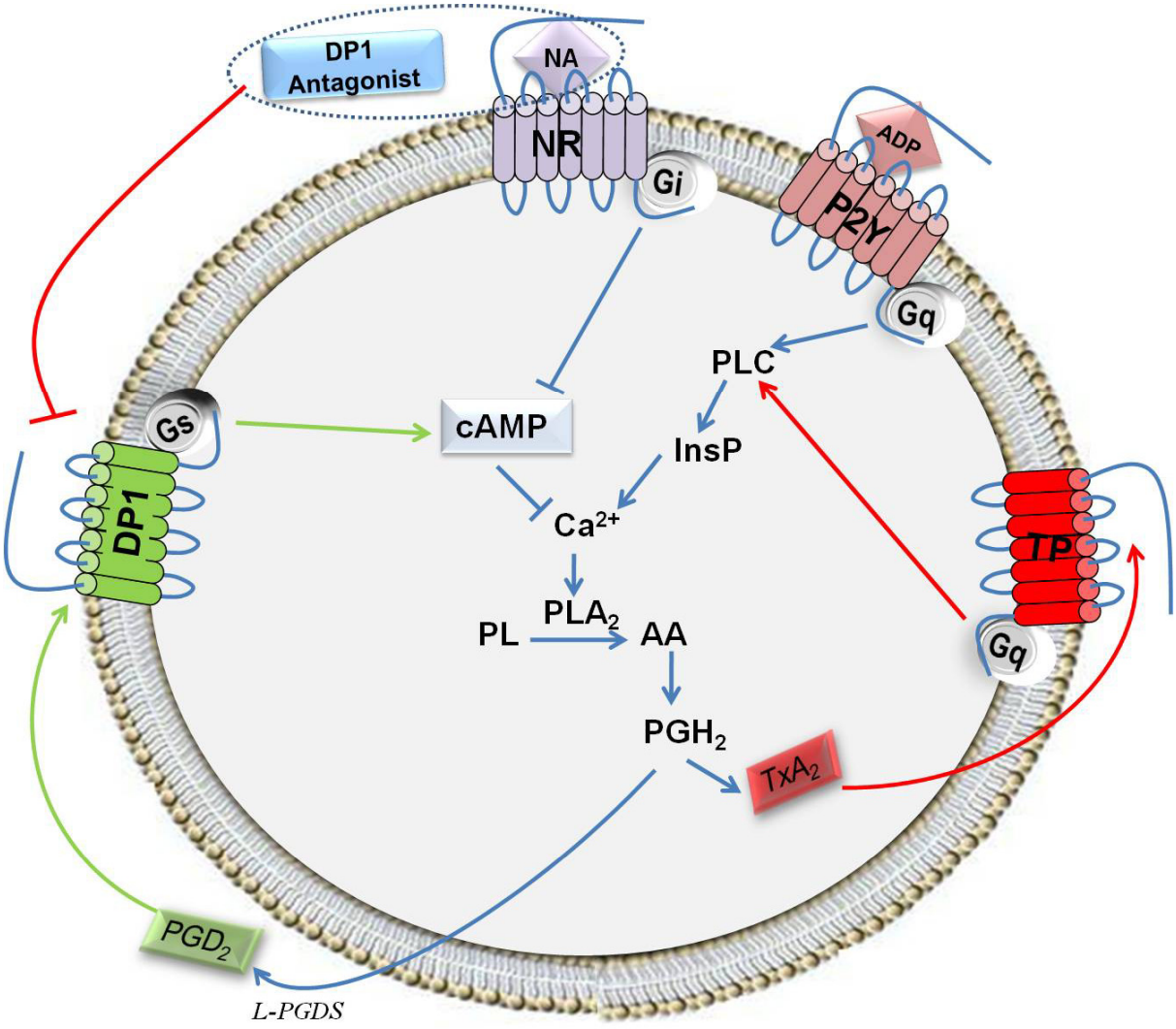

Supplement Fig 11 Effect of Niacin on human platelets